



Nov 6th, 12:00 AM - 12:00 AM

Calculation for Moment Capacity of Beam-to-Upright Connections of Steel Storage Pallet Racks

Tuo Wang

Xianzhong Zhao

Yiyi Chen

Follow this and additional works at: <https://scholarsmine.mst.edu/isccss>



Part of the [Structural Engineering Commons](#)

Recommended Citation

Wang, Tuo; Zhao, Xianzhong; and Chen, Yiyi, "Calculation for Moment Capacity of Beam-to-Upright Connections of Steel Storage Pallet Racks" (2014). *International Specialty Conference on Cold-Formed Steel Structures*. 1.

<https://scholarsmine.mst.edu/isccss/22iccfss/session08/1>

This Article - Conference proceedings is brought to you for free and open access by Scholars' Mine. It has been accepted for inclusion in International Specialty Conference on Cold-Formed Steel Structures by an authorized administrator of Scholars' Mine. This work is protected by U. S. Copyright Law. Unauthorized use including reproduction for redistribution requires the permission of the copyright holder. For more information, please contact scholarsmine@mst.edu.

Calculation for moment capacity of beam-to-upright connections of steel storage pallet racks

Tuo Wang¹, Xianzhong Zhao² and Yiyi Chen²

Abstract

Steel storage pallet rack structures are three-dimensional framed structures, which are widely used to store different kinds of goods. For the easy accessibility to stored products, pallet racks are not usually braced in the down-aisle direction. The down-aisle stability is mostly provided by the characteristics of beam-to-upright connections, and the characteristics of upright base connections. In this paper, calculation for moment capacity of beam-to-upright connections is carried out. A mechanical model is presented firstly. Based on the model, moment capacity is related to the failure capacity, directly determined by the failure mode, of the topmost tab of the beam-end-connector and the corresponding upright wall. Different methods to predict the failure capacity are derived for two types of failure modes, i.e. crack of tab and crack of upright wall. The new method has shown a satisfactory agreement with experimental results demonstrating the reliability of the model in predicting the moment capacity of beam-to-upright connections.

Introduction

Beam-to-upright connection is realized by connecting the beam to the upright through the beam end connector which is welded onto the end of beam and inserted into upright perforations by boltless tabs. A safety device is used to avoid pulling out of beam end connector from upright perforation in the presence of accidental uplift force. A typical beam-to-upright connection is shown in Figure 1.

¹ Doctoral Student, Tongji University, Shanghai, China

² Professor, Tongji University, Shanghai, China

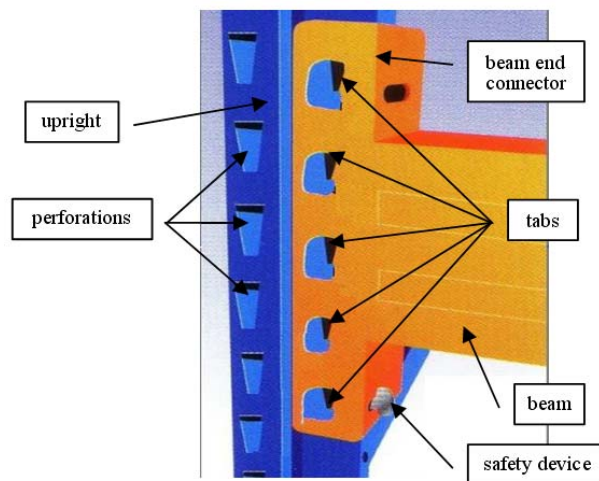


Figure 1 A typical beam-to-upright connection

Beam-to-upright connections play a fundamental role in the structural performance of racks. Generally besides the initial rotational stiffness, moment capacity is also a necessary parameter for a suitable definition of connection moment-rotation relationship. In the actual design of rack structures, according to European Standard (EN 15512 2009), the rotational stiffness of the connection used for design shall be obtained as the slope of a line through the origin which isolates equal areas between it and the moment-rotation curve, below the design moment M_{Rdc} , corrected for yield and thickness, as shown in Figure 2. M_{Rdc} is directly related to the moment capacity. In addition, researcher (Aguirre 2006) has presented the concept of fuse in the design of racks. It is assumed that the failure of the beam-to-upright connection is controlled entirely by the tabs, so the failure takes place at the beam end connector. The beam is more easily replaced, and the tabs act as fuses to prevent unwanted column failure. Implementation of the concept calls for identification of different component failure modes, and the moment capacities based on tab failure mode should be designed to be the minimum. Knowledge of the moment capacity of beam-to-upright connection is hence of vital importance.

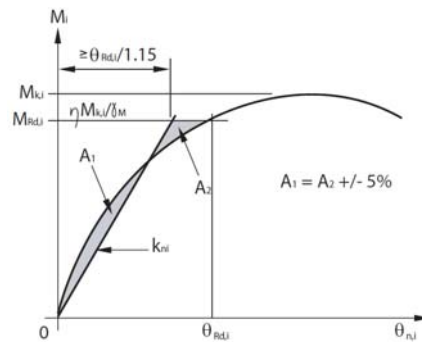


Figure 2 Derivation of connection stiffness used for design

Several researchers have studied the moment capacity the connection through test (Baldassino and Zandonini 2011; Krawinkler et al. 1979; Prabha et al. 2010). Some attempts were also made on numerical simulation (Markazi et al. 2001; Prabha et al. 2010), and the reliability of the numerical models strongly depends on their calibration against experimental results (Baldassino and Zandonini 2011). Comparing to experimental and numerical analysis, a convenient alternative is the theoretical analysis. To the authors' knowledge, there is only one paper concerned with theoretical investigation of pallet rack connections (Ślęczka and Kozłowski 2007), applying the so-call "component method" (Eurocode 3) to rack connections rigidly.

In this paper a mechanical model is established. By defining two failure modes, expressions are derived for the calculation of moment capacity. Comparison is made to a series of experimental results for a range of beam-to-upright connections of pallet racks.

Mechanical model for moment capacity

Deformation characteristics at failure

The deformation of the connection at failure is depicted in test photo of Figure 3. The failed connection presents obvious deformation characteristics. The deformation concentrates at the intersection of beam-end-connector and bottom beam flange (point P in Figure 3). The part of beam-end-connector above the point P deviates from the upright, with the tabs only connecting the beam-end-connector with the upright. The tabs distort seriously, rotating from the plane perpendicular to one leg of beam-end-connector to the plane almost

parallel to it, as shown in Figure 4.

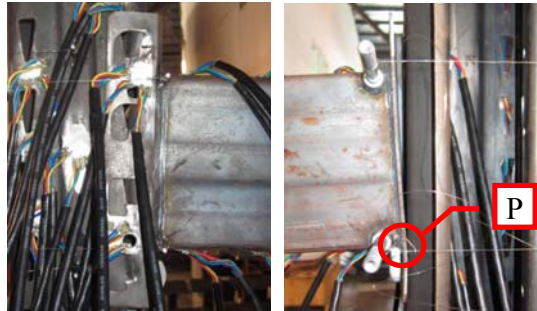


Figure 3 Front and back of a connection at failure

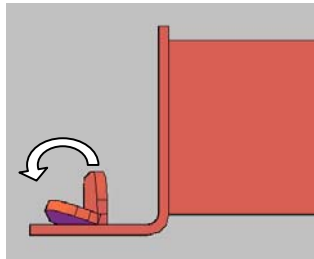


Figure 4 Distortion of the tab

According to the observed deformation characteristics in the test, a mechanical model for the moment capacity is presented as shown in Figure 5. Because the part of beam-end-connector beyond the top beam flange is very small, the two parts of the beam-end-connector divided by the point P are assumed to be rigid. The moment of connection is substituted by a couple of force F . Forces from the upright acted on the tabs of beam-end-connector are simulated by springs. The force F from the bottom beam flange transfers to the upright through the beam-end-connector leading to a reaction force R at the position of point P. A notional triangular distributed load is applied on the part of beam-end-connector beyond the bottom beam flange.

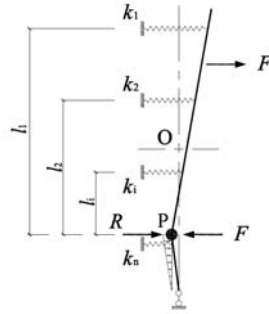


Figure 5 Mechanical model

Assumptions and principle of calculation

The imposed basic assumptions on the theoretical analysis for moment capacity are the following.

- (1) The bending moments about the point P resulted from reactions of upright to the beam-end-connector under the point P is small enough to be neglected.
- (2) The force for each spring above the point P is proportional to the deformation of the spring. Then the following equation can be obtained.

$$\frac{F_i}{F_j} = \frac{l_i}{l_j} \quad (1)$$

where F_i and l_i are the force and the arm of the i th spring, respectively.

The moment capacity M_u can be obtained by taking moments about the point P:

$$M_u = \sum_{i=1}^{n_u} F_i l_i \quad (2)$$

where n_u is the number of springs (or tabs) above the point P.

Substituting Eq. (1) into Eq. (2) can obtain the following equation for the moment capacity:

$$M_u = \sum_{i=1}^{n_u} F_1 \frac{l_i^2}{l_1} \quad (3)$$

where F_1 is the force of the topmost spring at the failure of connection.

Derivation of F_1 and M_u for different failure modes

Failure modes

The authors have carried experiment to investigate the behavior of the rack beam-to-upright connections (Zhao et al. 2014). All of the experimental moment-rotation curves reach the peak when the connection fails. The peak moment is then defined as moment capacity. There are two types of failure modes for the tested connections: crack of tab and crack of upright wall, which mode to occur depends on the relative strength of tab and upright wall. The tab construction is same for every connection specimen in the test, so the failure mode is decided by the thickness of upright wall. The crack of tab failure mode is predominant when the upright wall is 2.3mm or 2.5mm. For connections with a 1.8mm thickness upright, the failure mode is the crack of upright wall. If the thickness of upright wall is medium, i.e. 2.0mm, two types of failure modes may appear. The moment capacity obtained from experiment is listed in Table 1. Take 1.8C5-B120-4T as an example, 1.8C5 indicates the upright section is C5 type with the thickness of 1.8mm; B120 represents the depth of beam is 120mm and 4T means beam end connector has 4 tabs, i.e. the height of beam end connector is 200mm (4 times 50mm). It is easy to find that the results of three nominally identical connections in a group are very close.

Table 1 Experimental results of moment capacity

| Specimen ID | No. | Failure mode | $M_u(\text{kN}\cdot\text{m})$ | Mean |
|---------------|-----|-----------------------|-------------------------------|-------|
| 1.8C5-B120-4T | 1 | Crack of upright wall | 2.405 | 2.214 |
| | 2 | Crack of upright wall | 2.029 | |
| | 3 | Crack of upright wall | 2.208 | |
| 2.3C5-B120-4T | 1 | Crack of tab | 2.715 | 2.560 |
| | 2 | Crack of tab | 2.644 | |
| | 3 | Crack of tab | 2.322 | |
| 2.5C5-B120-4T | 1 | Crack of tab | 2.702 | 2.875 |
| | 2 | Crack of tab | 2.953 | |
| | 3 | Crack of tab | 2.971 | |
| 1.8C5-B105-4T | 1 | Crack of upright wall | 2.107 | 2.131 |
| | 2 | Crack of upright wall | 1.946 | |
| | 3 | Crack of upright wall | 2.341 | |
| 1.8C5-B145-4T | 1 | Crack of upright wall | 2.211 | 2.391 |
| | 2 | Crack of upright wall | 2.730 | |

| | | | | |
|---------------|---|-----------------------|-------|-------|
| | 3 | Crack of upright wall | 2.232 | |
| 1.8C5-B120-3T | 1 | Crack of upright wall | 1.646 | 1.427 |
| | 2 | Crack of upright wall | 1.267 | |
| | 3 | Crack of upright wall | 1.368 | |
| 1.8C5-B120-5T | 1 | Crack of upright wall | 2.713 | 2.829 |
| | 2 | Crack of upright wall | 2.875 | |
| | 3 | Crack of upright wall | 2.899 | |
| 1.8C4-B105-4T | 1 | Crack of upright wall | 1.977 | 1.999 |
| | 2 | Crack of upright wall | 2.067 | |
| | 3 | Crack of upright wall | 1.953 | |
| 2.0C4-B105-4T | 1 | Crack of tab | 2.140 | 2.172 |
| | 2 | Crack of upright wall | 2.178 | |
| | 3 | Crack of upright wall | 2.197 | |
| 1.8C4-B120-4T | 1 | Crack of upright wall | 2.396 | 2.419 |
| | 2 | Crack of upright wall | 2.388 | |
| | 3 | Crack of upright wall | 2.472 | |
| 1.8C4-B145-4T | 1 | Crack of upright wall | 2.517 | 2.427 |
| | 2 | Crack of upright wall | 2.586 | |
| | 3 | Crack of upright wall | 2.179 | |
| 1.8C4-B105-3T | 1 | Crack of upright wall | 1.487 | 1.473 |
| | 2 | Crack of upright wall | 1.558 | |
| | 3 | Crack of upright wall | 1.373 | |
| 1.8C4-B105-5T | 1 | Crack of upright wall | 2.194 | 2.217 |
| | 2 | Crack of upright wall | 2.284 | |
| | 3 | Crack of upright wall | 2.174 | |
| 1.8C3-B105-4T | 1 | Crack of upright wall | 1.898 | 1.969 |
| | 2 | Crack of upright wall | 2.007 | |
| | 3 | Crack of upright wall | 2.003 | |
| 1.8C3-B120-4T | 1 | Crack of upright wall | 2.210 | 2.178 |
| | 2 | Crack of upright wall | 2.175 | |
| | 3 | Crack of upright wall | 2.148 | |
| 1.8C3-B145-4T | 1 | Crack of upright wall | 2.191 | 2.258 |
| | 2 | Crack of upright wall | 2.327 | |
| | 3 | Crack of upright wall | 2.256 | |
| 1.8C3-B105-3T | 1 | Crack of upright wall | 1.348 | 1.329 |
| | 2 | Crack of upright wall | 1.267 | |
| | 3 | Crack of upright wall | 1.374 | |
| 1.8C3-B105-5T | 1 | Crack of upright wall | 2.341 | 2.274 |

| | | | | |
|--|---|-----------------------|-------|--|
| | 2 | Crack of upright wall | 2.178 | |
| | 3 | Crack of upright wall | 2.301 | |

Derivation of F_1 and M_u for crack of tab failure mode

For the failure mode of crack of tab, the mechanical analysis of the tab at the failure is shown in Figure 6. The crack probably appears at point C for the reason that point C is in the cold-formed region, material property of which has been changed adversely. The cross section of the tab at point C is subjected to a tensional effect combined with a bending moment. When the elastic theory applies, the strain at point C can be expressed as:

$$\varepsilon = \frac{1}{E} \left(\frac{F_1}{A_t} + \frac{F_1 e}{W_t} \right) \quad (4)$$

$$A_t = h_t t_t \quad (5)$$

$$W_t = \frac{1}{6} h_t^2 t_t \quad (6)$$

where $A_t = h_t t_t$ is the area of cross section, W_t is the modulus of section, e is the distance between the loading point of F_1 and the center of the cross section, h_t is the height of the cross section, t_t is the thickness of the tab and E is the elastic modulus.

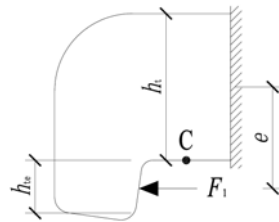


Figure 6 Mechanical analysis model for the tab

In an axial tensile coupon test, the energy absorbed by the steel at the fracture can be express by the energy absorbed per unit volume, value of which equals to the area enclosed by the stress-strain curve and abscissa axis, i.e. area of OKLO in Figure 7. According to energy equivalence (the area of OKLO equals to the area of OMNO), the fracture will occur at point M, where the elastic strain reaches k times yielding strain ε_y . The material property of the cold-formed

region of the tab is obtained by coupon test. Stress-strain curves for three coupons are shown in Figure 8. It is found that the average k value approaches to 3. So it can be assumed that the tab will crack when the elastic strain ε reaches $3\varepsilon_y$, i.e.

$$\varepsilon = 3\varepsilon_y = \frac{3f_{yt}}{E} \quad (7)$$

where f_{yt} is the yielding strength of the steel at the cold-formed region of the tab.

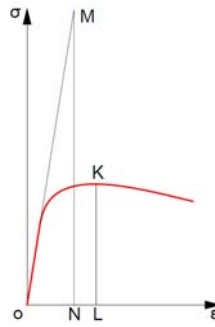


Figure 7 Stress-strain curve of a tensile test

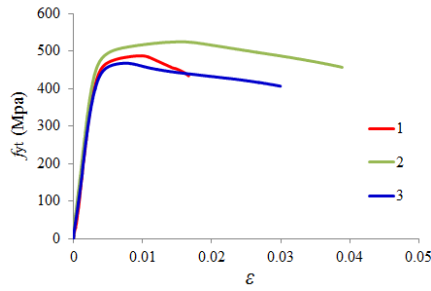


Figure 8 Coupon test results of cold-formed region of the tab

Using Eq. (4) to Eq. (7) to eliminate unnecessary quantities, F_1 can be expressed as:

$$F_1 = \frac{3f_{yt}h_t^2t_t}{h_t + 6e} \quad (8)$$

Substituting Eq. (8) into Eq. (3), the moment capacity for the failure mode of crack of tab can be expressed as:

$$M_u = \sum_{i=1}^{n_t} \frac{3f_{yt} h_i^2 t_i l_i^2}{h_i + 6e l_i} \quad (9)$$

The comparison between theoretical value M_u and experimental result M_E is listed in Table 2. When the thickness of upright wall is 2.0mm, the strength of the tab approaches to the strength of the upright wall. Connections may fail with crack of tab (specimen 2.0C4-B105-4T-1) or crack of upright wall (specimens 2.0C4-B105-4T-2/3). For the failure mode of crack of tab in the top three rows in Table 2, the theoretical values have a good agreement with the experimental results. For the failure mode of crack of upright wall in other rows in Table 2, although the comparison makes no sense, a conclusion can be drawn based on the ratio of M_u to M_E greater than 1.0, i.e. these connection will not fail in the failure mode of crack of tab, actual failure mode of which is the crack of upright wall, demonstrating the validity of the theoretical method in another sense.

Table 2 Comparison of theoretical values to test results

| Specimen ID | $M_u(\text{kN}\cdot\text{m})$ | $M_E(\text{kN}\cdot\text{m})$ | M_u/M_E |
|--------------------|-------------------------------|-------------------------------|-----------|
| 2.3C5-B120-4T | 2.640 | 2.560 | 1.031 |
| 2.5C5-B120-4T | 2.640 | 2.875 | 0.918 |
| 2.0C4-B105-4T -1 | 2.165 | 2.140 | 1.012 |
| 1.8C5-B120-4T | 2.640 | 2.214 | 1.192 |
| 1.8C5-B105-4T | 2.165 | 2.131 | 1.016 |
| 1.8C5-B145-4T | 2.983 | 2.391 | 1.247 |
| 1.8C5-B120-3T | 1.884 | 1.427 | 1.320 |
| 1.8C5-B120-5T | 3.345 | 2.829 | 1.182 |
| 1.8C4-B105-4T | 2.165 | 1.999 | 1.083 |
| 2.0C4-B105-4T -2/3 | 2.165 | 2.188 | 0.989 |
| 1.8C4-B120-4T | 2.640 | 2.419 | 1.091 |
| 1.8C4-B145-4T | 2.983 | 2.427 | 1.229 |
| 1.8C4-B105-3T | 1.752 | 1.473 | 1.189 |
| 1.8C4-B105-5T | 2.813 | 2.217 | 1.269 |
| 1.8C3-B105-4T | 2.165 | 1.969 | 1.100 |
| 1.8C3-B120-4T | 2.640 | 2.178 | 1.212 |
| 1.8C3-B145-4T | 2.983 | 2.258 | 1.321 |

| | | | |
|---------------|-------|-------|-------|
| 1.8C3-B105-3T | 1.752 | 1.329 | 1.318 |
| 1.8C3-B105-5T | 2.813 | 2.274 | 1.237 |

Derivation of F_1 and M_u for crack of upright wall failure mode

A mechanical analysis of the upright wall at the failure is shown in Figure 9. The force applied on the upright wall from the hook part of the tab is simplified to be an evenly distributed load q . The distribution length is equal to the length of the hook part, h_{te} , as shown in Figure 6. Assuming the strain of upright wall under the distributed load q is even in elastic range, i.e.:

$$\varepsilon = \frac{F_1}{Eh_{te}t_{up}} \quad (10)$$

where t_{up} is the thickness of upright wall.

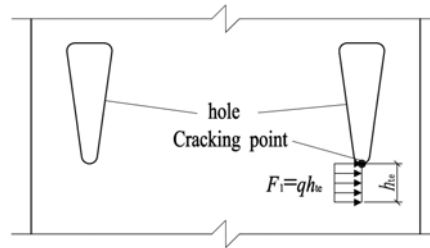


Figure 9 Mechanical analysis model for the upright wall

Similarly it is assumed that the upright wall will crack when the elastic strain ε reaches k times of the yielding strain ε_y of the steel, i.e.:

$$\varepsilon = k\varepsilon_y = k \frac{f_{yup}}{E} \quad (11)$$

where f_{yup} is the yielding strength of the steel at the cracking point of the upright wall as shown in Figure 9.

The expression for F_1 can be obtained from Eq. (10) and Eq. (11):

$$F_1 = kf_{yup}h_{te}t_{up} \quad (12)$$

Substituting Eq. (12) into Eq. (3), the moment capacity for the failure mode of crack of upright wall can be expressed as:

$$M_u = \sum_{i=1}^{n_u} k f_{yup} h_e t_{up} \frac{l_i^2}{l_1} \quad (13)$$

The value of k is difficult to determine using previous method for two reasons. Firstly the mechanical model in Figure9 is simple. Besides the tension effect, the upright wall is also subjected to a locally bearing effect from the hook part of the tab, which is not easy to be reflected in the model. Secondly the material property f_{yup} at the cracking point of the upright wall cannot be obtained by performing a coupon test because of small dimension. Therefore an inversion method is employed to get the value of k , i.e. calculating k from Eq. (13) where M_u is substituted by the experimental results M_E and f_{yup} by the yield strength f_{yp} of the plate part of upright profile approximately. The values of k for each specimen failed with crack of upright wall are listed in Table 3. The average value k_{avg} is 3.664. Meanwhile, an expression for k_{reg} is regressed as the function of the yield strength f_{yp} of the plate part of upright profile:

$$k_{reg} = 6.865 - 0.0096 f_{yp} \quad (14)$$

Table 3 The values of k for specimens failed with crack of upright wall

| Specimen ID | f_{yp} (MPa) | k |
|--------------------|----------------|-------|
| 1.8C5-B120-4T | 290 | 4.219 |
| 1.8C5-B105-4T | 290 | 4.783 |
| 1.8C5-B145-4T | 290 | 3.895 |
| 1.8C5-B120-3T | 290 | 3.681 |
| 1.8C5-B120-5T | 290 | 4.110 |
| 1.8C4-B105-4T | 370 | 3.516 |
| 2.0C4-B105-4T -2/3 | 342 | 3.748 |
| 1.8C4-B120-4T | 370 | 3.490 |
| 1.8C4-B145-4T | 370 | 3.099 |
| 1.8C4-B105-3T | 370 | 3.202 |
| 1.8C4-B105-5T | 370 | 3.002 |
| 1.8C3-B105-4T | 320 | 4.005 |
| 1.8C3-B120-4T | 320 | 3.633 |
| 1.8C3-B145-4T | 320 | 3.334 |

| | | |
|---------------|---------|-------|
| 1.8C3-B105-3T | 320 | 3.341 |
| 1.8C3-B105-5T | 320 | 3.561 |
| | Average | 3.664 |

The theoretical values of moment capacity M_u based on both k_{avg} and k_{reg} are compared with the experimental results M_E as listed in Table 4. The results using the value of k from regression seem to have a better agreement with the experimental results.

Table 4 Comparison of theoretical values to test results for different k

| Specimen ID | $M_u(kN \cdot m)$ | | $M_E(kN \cdot m)$ | M_{u1}/M_E | M_{u2}/M_E |
|------------------|-------------------|--------------------|-------------------|--------------|--------------|
| | $M_{u1}(k_{avg})$ | $M_{u2}(k_{reg})$ | | | |
| C5-B120-4T | 1.991 | 2.217 | 2.214 | 0.899 | 1.001 |
| C5-B105-4T | 1.633 | 1.819 | 2.131 | 0.766 | 0.853 |
| C5-B145-4T | 2.249 | 2.505 | 2.391 | 0.941 | 1.048 |
| C5-B120-3T | 1.420 | 1.582 | 1.427 | 0.995 | 1.109 |
| C5-B120-5T | 2.522 | 2.809 | 2.829 | 0.891 | 0.993 |
| C4-B105-4T | 2.083 | 1.884 | 1.999 | 1.042 | 0.942 |
| C4*-B105-4T -2/3 | 2.139 | 2.091 | 2.188 | 0.978 | 0.956 |
| C4-B120-4T | 2.540 | 2.297 | 2.419 | 1.050 | 0.949 |
| C4-B145-4T | 2.869 | 2.595 | 2.427 | 1.182 | 1.069 |
| C4-B105-3T | 1.685 | 1.524 | 1.473 | 1.144 | 1.035 |
| C4-B105-5T | 2.706 | 2.447 | 2.217 | 1.220 | 1.104 |
| C3-B105-4T | 1.801 | 1.865 | 1.969 | 0.915 | 0.947 |
| C3-B120-4T | 2.197 | 2.274 | 2.178 | 1.009 | 1.044 |
| C3-B145-4T | 2.482 | 2.569 | 2.258 | 1.099 | 1.138 |
| C3-B105-3T | 1.458 | 1.509 | 1.329 | 1.097 | 1.135 |
| C3-B105-5T | 2.340 | 2.423 | 2.274 | 1.029 | 1.065 |
| | | Average | | 1.014 | 1.022 |
| | | Max | | 1.220 | 1.138 |
| | | Min | | 0.766 | 0.853 |
| | | Standard Deviation | | 0.119 | 0.080 |

From the above, M_u can be calculated according to:

$$M_u = \min \left(\sum_{i=1}^{n_b} \frac{3f_{yt} h_i^2 t_i}{h_i + 6e} \frac{l_i^2}{l_i}, \sum_{i=1}^{n_u} k_{f_{yup}} h_{ie} t_{up} \frac{l_i^2}{l_i} \right) \quad (15)$$

Conclusions

Moment capacity is determined by the failure mode. Based on mechanical models, analysis expressions for the moment capacity of beam-to-upright connections of steel storage pallet racks have been developed theoretically. The expressions have been compared with a series of experimental results to determine their accuracy.

References

- Aguirre, C. (2006). "Seismic behavior of rack structures." *Journal of Constructional Steel Research*, 61(5), 607-624.
- Baldassino, N., and Zandonini, R. (2011). "Design by testing of industrial racks." *Advanced Steel Construction*, 7(1), 27-47.
- EN 15512. (2009). *Steel static storage systems-Adjustable pallet racking systems-Principles for structural design*, European Committee for Standardization (CEN), Brussels, Belgium.
- Eurocode 3. (2005). *Design of steel structures- Part 1.8: Design of joints*, European Committee for Standardization (CEN), Brussels, Belgium.
- Krawinkler, H., Cofie, N. G., Astiz, M. A., and Kircher, C. A. (1979). "Experimental study on the seismic behavior of industrial storage racks." The John A. Blume Earthquake Engineering Center, Department of Civil and Environmental Engineering, Stanford University, Report No.41, California.
- Markazi, F. D., Beale, R. G., and Godley, M. H. R. (2001). "Numerical modelling of semi-rigid boltless connector." *Computers & Structures*, 79(26-28), 2391-2402.
- Prabha, P., Marimuthu, V., Saravanan, M., and Jayachandran, S. A. (2010). "Evaluation of connection flexibility in cold formed steel racks." *Journal of Constructional Steel Research*, 66(7), 863-872.
- Ślęczka, L., and Kozłowski, A. (2007). "Experimental and theoretical investigations of pallet racks connections." *Advanced Steel Construction*, 3(2), 607-627.
- Zhao, X. Z., Wang, T., Chen, Y. Y., and Sivakumaran, K. S. (2014). "Flexural behavior of steel storage rack beam-to-upright connections." *Journal of Constructional Steel Research*, submitted.